X-ray spectral components in the hard state of GRS 1915+105 : origin of the 0.5 − 10 Hz QPO

A.R. Rao[1], S. Naik[1], S.V. Vadawale[1] and Sandip K. Chakrabarti[2]

[1]Tata Institute of Fundamental Research, Homi Bhabha Road, Mumbai(Bombay) 400 005, India
[2]S.N. Bose National Centre for Basic Sciences, Salt Lake, Calcutta 7000091, India

Abstract. We investigate the origin of the ubiquitous 0.5 − 10 Hz QPO in the Galactic microquasar GRS 1915+105. Using the archival X-ray data from RXTE, we make a wide band X-ray spectral fitting to the source during a low-hard state observed in 1999 June. We resolve the X-ray spectra into three components, namely a multi-color disk component, a Comptonised component and a power-law at higher energies. This spectral description is favored compared to other normally used spectra like a cut-off power law, hard components with reflection etc. We find that the 0.5 − 10 Hz QPO is predominantly due to variations in the Comptonised component. We use this result to constrain the location of the various spectral components in the source.

Key words: X-rays: stars – accretion, accretion disks – black hole physics – stars: winds, outflows – stars: individual (GRS 1915+105)

1. Introduction

The Galactic microquasar GRS 1915+105 is a bright X-ray source and it is a subject of intense study in all wavelengths (see Mirabel & Rodriguez 1999, and references therein). It has been exhibiting a multitude of types of X-ray variability characteristics ranging from a quasi-stable high frequency QPO at 67 Hz (Morgan, Remillard, & Greiner 1997) to long durations of stable emission modes (Belloni et al. 2000). One of the interesting features of this source is the detection of a stable, narrow, and intense QPO in the frequency range of 0.5 − 10 Hz (Agrawal et al. 1996; Morgan & Remillard 1996). Chen, Swank, & Taam (1997) found that this QPO emission is a characteristic feature of the hard branch and it is absent in the soft branch. Paul et al. (1998) found that the 0.5 − 10 Hz QPO

traces the change of state from a "flaring state" to a low-hard state quite smoothly along with other X-ray characteristics like the low frequency variability. Trudolyubov, Churazov, & Gilfanov (1999b) studied the low state and state transitions using the RXTE data and concluded that the QPO centroid frequency is correlated with the spectral and timing parameters. Muno, Morgan, & Remillard (1999) found that the 0.5 − 10 Hz QPO can be used as a tracer of the spectral state of the source and the source mainly stays in two states: the spectrally hard state with the QPO and the soft state without the QPO. Another interesting feature of the 0.5 − 10 Hz QPO is that it is also found during the brief episodes of 'off' states when the source teeters between 'off' and 'on' states (Belloni et al. 1997; Yadav et al. 1999).

The large rms amplitude (about 10%), narrow width and the relative stability over considerably long durations makes it difficult to explain the 0.5 − 10 Hz QPO on the basis of the inner disk oscillations in the accretion disk. Chakrabarti & Manickam (2000) showed that even in the spectrally harder states, not all the photons participated in QPOs. They found that, 0-4 keV soft photons showed little or no sign of QPO while 4-13 keV photons exhibited QPO. They interpret this as due to the oscillation of the region responsible for the hard radiation, i.e., the post-shock region. They also detected a correlation between the average frequency of the QPO and the duration of the 'off' states. Similar correlation with centroid frequencies were also found by Trudolyubov, Churazov, & Gilfanov (1999a).

In this *Letter*, we perform a detailed X-ray spectroscopy of the source using the RXTE data archives. We find a better way to quantify the nature of the photons which participated in QPOs. We show that the entire spectrum can be split into a disk blackbody component, a thermal Compton component and an additional hard component and only the Comptonised component participates in QPOs.
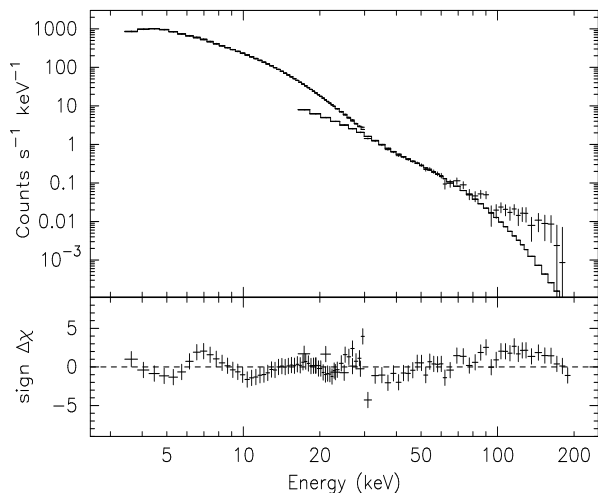
Fig. 1. The observed count rate spectrum of GRS 1915+105 obtained from RXTE PCA and HEXTE on 1999 June 7. The error bars are smaller than the symbol sizes in the low energies. A best-fit model consisting of a disk blackbody and a cutoff power-law is shown as histogram and the residuals are shown in the bottom panel of the figure.

2. Analysis and results

2.1. Data selection

The $0.5 - 10$ Hz QPO is detected during the low hard states as well as during the low state of bursts (Muno et al. 1999). The long duration hard states are classified as the χ state in Belloni et al. (2000), who have made a comprehensive study of RXTE PCA observations on GRS 1915+105 using the total count rates and color-color diagrams. The χ state is further divided into χ_1 to χ_4 states depending on the count rate and color. The χ_3 state is also found to be associated with high radio emission - the "plateau state" (Fender et al. 1999). Each of these steady hard states stays for a long duration (a few days to a few months - see Belloni et al. 2000) and during a given steady state the spectral and temporal behaviors are similar. To quantify the relation between the QPO emission and the spectral parameters, we have selected one observation in the χ_3 state of the source, obtained on 1999 June 7. A detailed spectral and temporal analysis of all the steady hard states of the source will be presented elsewhere (Vadawale et al. 2000).

The χ_3 state in 1999 June lasted from June 2 to June 7. The source exhibited a huge radio flare immediately thereafter (see Naik et al. 2000 for details of the source properties during this flare episode). We have selected the RXTE X-ray spectral data obtained on 1999 June 7, just prior to this radio flare. The observation PID is 40703-01-17-01. We have made a combined analysis of the data obtained from RXTE PCA (Jahoda et al. 1996) and HEXTE (Rothschild et al. 1998). We have generated the 129 chan-
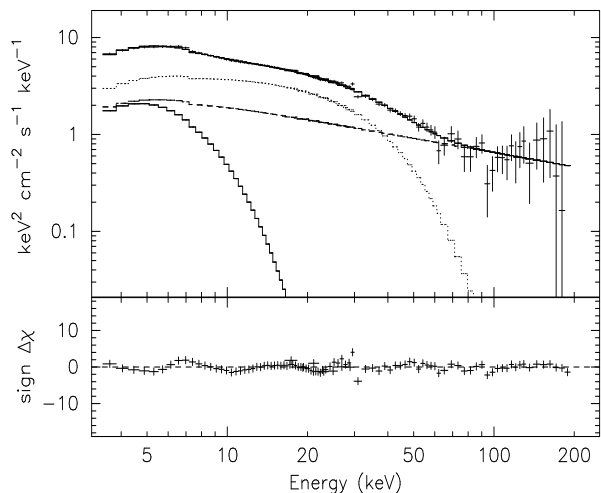

Fig. 2. The unfolded spectrum (in νF_ν units) shown for the spectrum of Figure 1. The best-fit model consists of a disk blackbody (continuous line), a thermal Compton spectrum (dotted line) and a power-law (dashed line).

nel energy spectra from the Standard 2 mode of the PCA. Standard procedures for data selection, background estimation and response matrix generation have been applied. PCA consists of five units (called PCUs) and during the present observation only three of them (PCU numbers 0, 2, and 3) were active. Data from the three units are added together. For the HEXTE, standard 2 as well as the event mode data have been used. Systematic errors of 2 % have been added to the PCA spectral data. For the present analysis, we use data from only the HEXTE Cluster 0, which has better spectral response.

2.2. Spectral analysis

To understand the systematic errors involved in the data, we have analyzed the spectra obtained on the Crab nebula. We have also made a systematic analysis of the Crab data obtained from other missions like Beppo-SAX and ASCA. We find that HEXTE Cluster 0 gives satisfactory values of χ^2 when a simultaneous fit to the Crab is made using various missions (see Vadawale et al. 2000 for details). Attempt to fit the PCA and HEXTE data simultaneously gave unacceptable values of χ^2 particularly due to a large excess in low energies in PCA (this was noted by Gierlinski et al. 1999). With the addition of a 2% systematic error, the $3 - 30$ keV PCA spectrum of Crab gives statistically acceptable simultaneous fit with the HEXTE spectrum. We, therefore, have selected only the $3 - 30$ keV spectrum from the PCA with a systematic error of 2% for the present analysis.

We have fitted the energy spectrum of the source using the standard black hole accretion model (see Muno et al. 1999) consisting of disk-blackbody and power-law with

absorption by intervening cold material parameterized as equivalent Hydrogen column density, N_H. The value of N_H has been kept fixed at 6×10^{22} cm^{-2}. A simultaneous fit to the PCA (in the energy range of 3.5 – 30 keV) and HEXTE (in the energy range of 16.5 – 190 keV) data was carried out, keeping the relative normalization as a free parameter. We find a reasonably good fit with a value of reduced χ^2 (χ^2_ν) of 2.2 for 96 degrees of freedom (dof), but the derived value of temperature was unrealistically high (6.4 keV). Restricting the temperature to less than 3 keV resulted in a χ^2_ν of greater than 11.7. It was also noted by Muno et al. (1999) that the low hard states with the radio "plateau" emission show very high temperature and low inner disk radius. A cut-off power-law model along with the disk blackbody gives χ^2_ν of 1.7. The resultant fitted spectrum along with the residuals normalized to the errors, are given in Figure 1. A strong excess above 70 keV is noticeable in the spectrum. We have attempted to model this component as an additional power-law. It gives an acceptable value of χ^2_ν of 1.2. But the value of the photon index of this additional power-law is 0.5, which gives unrealistically high values of emission above the RXTE range of 200 keV. Hence we have explored other possible models to fit the spectrum.

It was shown by Chitnis et al. (1998) that the hard state of Cygnus X-1 can be described by a model consisting of a disk blackbody and a thermal Compton spectrum (Sunyaev & Titarchuk 1980), with an additional hard component. We have attempted to fit the GRS 1915+105 spectrum using a model consisting of a disk blackbody (diskbb), a thermal-Compton spectrum (CompST) and a power-law, along with the fixed cold absorption. A satisfactory fit to the data is obtained with χ^2_ν value of 1.2. The resultant unfolded spectrum, in νF_ν units, along with the residuals, is shown in Figure 2. The individual model components are also shown in the figure. The derived parameters are: 1.4±0.1 keV (disk temperature), 7.0±1.3 keV (CompST temperature), 6.2±1.3 (CompST optical depth τ), and 2.5±0.4 (power-law photon index). The relative normalization of HEXTE with respect to PCA is derived to be 0.65±0.01 (which is the same as the value obtained from the analysis of data on the Crab nebula). The quoted errors are nominal 90% ($\chi^2 + 4.6$ for 2 degrees of freedom).

2.3. Timing analysis

For the timing analysis we have used the 1.5 – 5.5 keV and 5.5 – 12.7 keV light curves (with a time resolution of 16 ms) from all the 3 active PCUs. Power density spectra (PDS) were generated for 256 bins and then co-added. Contribution from Poisson counting statistics has been subtracted. A QPO is clearly detected at a frequency of 2.9 Hz, along with its first harmonic and the PDS is very flat below ∼0.5 Hz. The centroid frequencies of the QPO and its first harmonics were determined by fitting Lorentzian functions. The frequencies derived for the low energy data
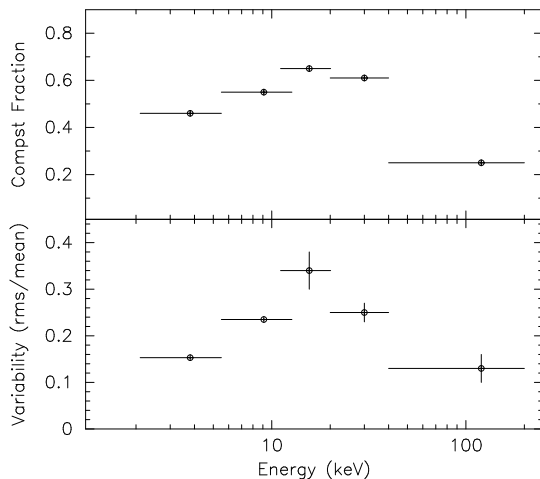

Fig. 3. The rms variability in 1 – 4 Hz is plotted as a function of energy is shown in the bottom panel. The first two data points are from PCA and the last three are from HEXTE. In the top panel the variation in the contribution to the energy spectrum from the thermal Compton component is shown to highlight the close similarity between the temporal variability and the spectral component.

are 2.87±0.01 Hz and 5.36±0.05 Hz, while that for the high energy data are 2.87±0.01 Hz and 5.17±0.08 Hz, respectively. The rms variation in the QPO peaks in the low energy data are 10% and 5.3%, respectively, and the same for the high energy data are 16% and 7.1%, respectively.

The increase of the rms in the QPO with energy has been noted earlier (Muno et al. 1999), and comparing with Figure 2, it is quite suggestive that the CompST contribution in the energy spectrum also increases with energy. To further investigate this, we have taken the event mode data for HEXTE and generated PDS for 3 energy ranges namely 11.3 – 20 keV, 20 – 40 keV and 40 – 200 keV. The total power in the PDS between 1 Hz – 4 Hz are calculated. These values are shown as a function of energy in the bottom panel of Figure 3. We have calculated the relative contribution of the CompST component to the energy spectrum in different energy bins, and these are plotted in the top panel of Figure 3. There is a strong correlation between the relative strengths of the CompST component and the 1 – 4 Hz rms variability, suggesting that the CompST component is responsible for the variability.

We have also extracted high time resolution light curve of the three model components. For this purpose, three energy ranges are considered: the two energy bands from the PCA as explained earlier, and 11.3 – 40 keV range from the HEXTE. Light curves are generated at 64 ms time resolution. The relative contributions of the three components are calculated for each of the energy bins from the fit to the energy spectra. By assuming that the time variability is mainly due to variations in the normaliza-
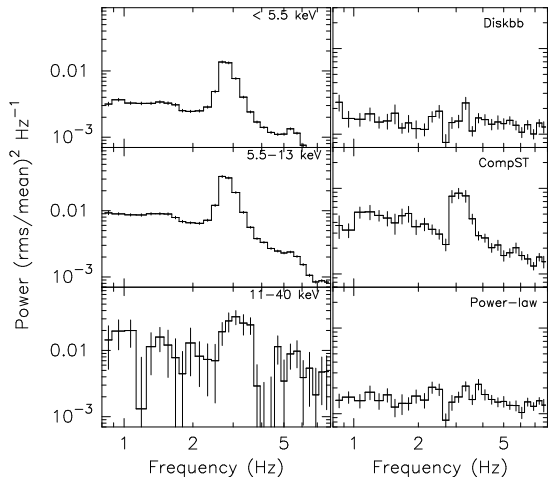
Fig. 4. The PDS in 3 energy ranges are shown in the left panels of the figure. In the right panels PDS generated after converting the light curves in 3 energy channels into light curves in three spectral components are shown.

tions of the spectral components rather than the spectral parameters, the normalization constant for each spectral bin are calculated by a χ^2 grid search. Light curves were created for each of the spectral components with a time resolution of 64 ms. PDS were calculated for the three decomposed spectral components and these are shown in the right panel of Figure 4.

The left panel of Figure 4 shows the PDS in the 3 energy bands, where the QPO is clearly seen. The QPO feature is very prominent for the CompST component and undetectable for the disk blackbody and the power-law components. This strongly indicates that the CompST component in the energy spectrum is primarily responsible for the QPO generation.

3. A possible model for the QPO

In the present *Letter*, we have shown very conclusively that only the Comptonised photons participate in QPOs. Chakrabarti & Manickam (2000) had concluded that the emission from the post-shock region is responsible for the QPOs, by crudely splitting the light curves into soft photons (0-4) keV and hard photons (4-13) keV. Chakrabarti & Titarchuk (1995) and Chakrabarti (1997) while computing steady state spectrum from the disk showed that the post-shock region re-emit photons intercepted from the Keplerian disk after inverse Comptonisation by the post-shock flow. They also conjectured that shock oscillations would produce QPOs in hard radiations and not in soft radiations. One way to reconcile the present observation is therefore to imagine that even when the oscillation is 'on', the two component advective flow (TCAF) model as proposed by Chakrabarti & Titarchuk (1995) and Chakrabarti (1997) remains valid. Oscillation of shocks

vary the puffed-up post-shock region (Molteni, Sponholz, & Chakrabarti, 1996) and intercept variable amount of soft-photons from the pre-shock Keplerian region which emits blackbody radiation. Since the fractional change in the number of intercepted (and thus emitted) photons in the post-shock region is very large compared to that from the Keplerian flow, QPO is strongest in the Comptonised photons and very nearly absent in the blackbody photons. Since Keplerian disks do not produce shocks by definition, it must be surrounded by the sub-Keplerian flows which does. This was the basis of the two-component advective flow models of Chakrabarti & Titarchuk (1995) and Chakrabarti (1997). What is new in our present paper is that we show not *all* the hard photons participate in QPOs, but only those produced by Comptonisation. This further strengthens the shock oscillation models.

4. Discussion and conclusions

The aim of the present work is to pin-point the source of QPOs by making a detailed X-ray spectral analysis. It is known that the 0.5 – 10 Hz QPO is closely related to the hard power-law component and it is used as a tracer to determine the spectral states (Muno et al. 1999). To completely identify the QPO phenomena with a particular spectral emission component, a careful fitting of the X-ray spectrum was required. The difficulty of fitting the X-ray spectrum using RXTE PCA has been highlighted by Gierlinski et al. (1999). We have circumvented this problem by relying primarily on the HEXTE data (which was validated by the Crab analysis) and using PCA at a lower weight by adding a systematic error of 2%. Hence the exact parameters of the low energy components like the black-body temperature etc. need further confirmation. But, the existence of the various hard X-ray spectral components is much more secure. The spectral analysis shows that the model presented in the present work is acceptable. We have explored other possible models for the spectra like combination of power-law, cut-off power-law etc. along with reflection components. We find that disk blackbody with CompST and power law is preferred by the data compared to all other models.

The existence of a separate power law is a new feature brought out from the present analysis. In similar states (radio loud hard state) Muno et al. (1999) found that the spectrum can be fitted by a disk blackbody and a power law. We find that a temperature of >4 keV and inner disk radius of ∼1 km derived by such a model is quite unrealistic.

We find that the high energy power-law feature is a generic feature in the χ_3 state of the source, when the radio emission is high (the "plateau" state). It is quite possible that this power-law X-ray feature is an extension of the flat-spectrum radio emission which is identified with a jet of core size 10 AU (Dhawan et al. 2000). A systematic search for such a power-law feature and an at-

tempt to identify this with the radio emission is currently in progress (Vadawale et al. 2000).

The fact that the CompST component in the energy spectrum is responsible for the QPO generation agrees with the hypothesis that the QPO is generated by the oscillation of the shock front. This picture explains several of the correlations reported in the literature for the 0.5 – 10 Hz QPO in GRS 1915+105. When the shock front comes closer to the black hole, the QPO frequency should increase and so should the blackbody flux, as has been observed (Markwardt et al. 1999; Chen et al. 1997). When the accretion rate increases, there will be a large number of soft photons to cool the Compton cloud. This effectively removes the Compton region in the soft state and the 0.5 – 10 Hz QPO is not seen. Recently Reig et al. (2000) have detected phase lags of both signs between soft and hard photons during the hard phase of GRS 1915+105. The lags were up to $\sim$0.3 radians. Such large lags with different signs are difficult to reconcile with any simple models of Comptonisation. It could be, however, due to the different shapes of the QPO profile at different energies, which appear as phase lags.

References

Agrawal, P. C., et al. 1996, IAU Circ. 6488

Belloni, T., et al. 1997, ApJ, 488, L109

Belloni, T., Klein-Wolt, M., Mendez, M., van der Klis, M., & van Paradijs, J. 2000, A&A, 355, 271

Chakrabarti, S. K. 1997, ApJ, 484, 313.

Chakrabarti, S. K., & Manickam, S. G. 2000, ApJ, 531, L41.

Chakrabarti, S. K., & Titarchuk, L. G. 1995, ApJ, 455, 623.

Chen, X., Swank, J. H., & Taam, R. E. 1997, ApJ, 477, L41

Chitnis, V.R., Rao, A.R., & Agrawal, P.C. 1998, A&A, 331, 251

Dhawan, V., Mirabel, I.F., & Rodriguez, L.F. 2000, ApJ, in press, astro-ph/0006086

Fender, R. P., Garrington, S. T., McKay, D. J., Muxlow, T. W. B., Pooley, G. G., Spencer, R. E., Stirling, A. M., & Waltman, E. B. 1999, MNRAS, 304, 865

Gierlinski, M., Zdziarski, A. A., Poutanen, J, Coppi, P. S., Ebisawa, K., & Johnson, W. N. 1999, MNRAS, 309, 496

Jahoda, K., et al. 1996, SPIE, 2808, 59

Markwardt, C.B., Swank, J.H., & Taam, R.E. 1999, ApJ, 513, L37

Mirabel, I.F. & Rodriguez, L.F. 1999, ARA&A, 37, 409

Morgan, E. H. & Remillard, R. A. 1996, IAU Circ., 6392

Molteni, D., Sponholz, H., & Chakrabarti, S. K. 1996, ApJ, 457, 805.

Morgan, E. H., Remillard, R. A., & Greiner, J. 1997, ApJ, 482, 993

Muno, M.P., Morgan, E.H., & Remillard, R. A. 1999, ApJ, 527, 321.

Naik, S. et al. 2000, ApJ, submitted

Paul, B., et al. 1998, A&AS, 128, 145

Reig, P., Belloni, T., van der Klis, M., Mendez, M., Kylafis, N., & Ford, E.C. 2000, astro-ph/0001134

Rothschild, R.E., et al. 1998, ApJ, 496, 538

Sunyaev, E.A., & Titarchuk, L. 1980, A&A, 86, 121

Trudolyubov, S., Churazov, E., & Gilfanov, M. 1999a, A&A, 351, L15

Trudolyubov, S., Churazov, E., & Gilfanov, M. 1999b, Ast. L., 25, 718

Vadawale, S.V., et al., 2000, in preparation

Yadav, J. S., Rao, A. R., Agrawal, P. C., Paul, B., Seetha, S., & Kasturirangan, K. 1999, ApJ, 517, 935